The 48 Layer COMMA-LIM Model: Model description, new Aspects, and Climatology

K. Fröhlich, A. Pogoreltsev and Ch. Jacobi

Zusammenfassung
COMMA-LIM (Cologne Model of the Middle Atmosphere - Leipzig Institute for Meteorology) ist ein 3D-mechanistisches Gitterpuktsmodell, welches sich von ca. 0 bis 135 km in logarhitmischen Druckkordinaten $z = -H \ln(p/p_0)$ erstreckt, wobei H=7 km und p_0 den Referenzdruck am unteren Rand bezeichnet. Die vertikale Auflösung von COMMA-LIM wurde auf 48 Schichten erhöht. Zugleich wurde die Beschreibung des Strahlungsprozesses verbessert, zusammen mit den Beiträgen zur Temperaturbilanz durch atmosphärische Wellen und Turbulenz. Weitere Veränderungen betreffen die numerische Realisation der horizontalen Diffusion und des Filterproblems. Die Beschreibung ist unterteilt in den dynamischen Teil und die Strahlungsbeträge. Die jahreszeitlichen Klimatologien werden vorgestellt und diskutiert.

Summary
COMMA-LIM (Cologne Model of the Middle Atmosphere - Leipzig Institute for Meteorology) is a 3D-mechanistic gridpoint model extending up from 0 to 135 km with a logharithmic vertical coordinate $z = -H \ln(p/p_0)$, where H=7 km and p_0 is the reference pressure at lower boundary. The resolution of the 24 layer version has been increased to 48 layers and several improvements are made in the parameterisation of radiative processes, heating/cooling due to atmospheric waves and turbulence, as well as in the numerical realization of the horizontal diffusion and filtering. This description is divided into the section describing the changes in the dynamical part and the modifications in radiation routines. After all, the seasonal climatologies will be shown and discussed to demonstrate what the COMMA-LIM is capable of reproducing.

1 Dynamics

The prognostic equations for horizontal wind components and temperature are the Navier-Stokes and energy equations, respectively. Hydrostatic assumption and continuity equation are used for diagnosis (for details see Lange, 2001). As a lower boundary condition a zonally averaged geopotential height at 1000 hPa is included which was obtained from 11-year averaged monthly mean UKMO assimilated data. At the upper boundary the vertical velocity is set to zero. The Rayleigh friction and Newtonian cooling coefficients increase near the upper boundary to suppress the reflection of planetary waves and tides. The different contribution terms are improved, such as impacts due to atmospheric waves, ion drag and turbulence/diffusion.

1.1 Gravity Waves

The gravity wave (GW) parameterising scheme is based on the Lindzen approach, which states that wave breaking occurs when the isentropes first become vertical, with $\partial\theta/\partial z = 0$, thus implying a loss of static stability and the onset of turbulence and mixing [see also Andrews et al. (1987)]. This assumption is improved taking into account possible multiple breaking levels and wave propagation between layers where the wave is saturated, as well as heating/cooling effects due to GW dissipation. The parameterisation is based on an analytical solution (WKB approximation) of the vertical structure equation for the GW in the atmosphere with realistic arbitrary background wind and realistic radiative damping. The Eddy diffusion coefficient is estimated using the idea of GW breaking due to instability proposed by Lindzen (1981).

WKB solution

The linearized set of equations describing the propagation of GW can be written as follows:

$$-i\omega^+ u' - \frac{1}{k_x}\frac{\partial\omega^+}{\partial z}w' + ik_x\phi' = \frac{1}{\rho}\frac{\partial}{\partial z}\rho D\frac{\partial u'}{\partial z}, \tag{1}$$

$$\frac{\partial\phi'}{\partial z} = \theta'\frac{R}{H}\exp(-\frac{\kappa z}{H}), \tag{2}$$

$$ik_x u' + \frac{1}{\rho}\frac{\partial}{\partial z}\rho w' = 0, \tag{3}$$

$$-i\omega^+\theta' + \frac{\partial\bar{\theta}}{\partial z}w' = \frac{1}{\rho}\frac{\partial}{\partial z}\rho\frac{D}{Pr}\frac{\partial\theta'}{\partial z} - \alpha\theta', \tag{4}$$

where u' and w' are the perturbed horizontal (along the horizontal component of the wave vector) and vertical (positive) velocities, ϕ' is the gravity wave geopotential, and θ' is the perturbed potential temperature; $z = -H\ln(p/p_s)$ is the vertical coordinate, p_s is a standard reference pressure; $\omega^+ = \omega - k_x(\bar{u}\cos\vartheta + \bar{v}\sin\vartheta)$ is an intrinsic frequency of a gravity wave, k_x is the horizontal wave number, $\bar{u}$ and $\bar{v}$ are zonal and meridional components of the background wind, ϑ is the azimuth of GW propagation; D and α are the eddy diffusion and Newtonian cooling coefficients, H is the scale height, $\rho(z) = \rho_s\exp(-z/H)$ is a reference density; R is the gas constant for dry air, $\kappa = R/c_p$, c_p is the specific heat at constant pressure, and Pr is turbulent Prandtl number. Overbars denote the background values averaged over a wave period.

Without dissipation ($D = \alpha = 0$) the set of equations (1)-(4) can be reduced to one equation for the complex amplitude of the perturbed vertical velocity $W(z) = w'(x,z,t)\exp[-i(k_x x - \omega t)]$

$$[\frac{d^2}{dz^2} + \mathcal{L}\frac{d}{dz} + \mathcal{M}]W(z) = 0, \tag{5}$$

where

$$\mathcal{L} = -\frac{1}{H}, \qquad \mathcal{M} = \frac{N^2 k_x^2}{\omega^{+2}} - \frac{1}{H}\frac{1}{\omega^+}\frac{\partial\omega^+}{\partial z} - \frac{1}{\omega^+}\frac{\partial^2\omega^+}{\partial z^2},$$

and $N^2 = R(\partial\bar{T}/\partial z + \kappa\bar{T}/H)/H$ is the Brunt- Väisälä frequency squared.

In the case of slowly varying media equation (5) has an approximate analytical solution, which can be written as follows (the so called WKB solution):

$$W(z) = W(0)[k_z(0)/k_z(z)]^{1/2} e^{\pm i\int_0^z k_z(z')dz'} e^{-\frac{1}{2}\int_0^z \mathcal{L}(z')dz'}, \tag{6}$$

where the vertical wavenumber squared is:

$$k_z^2 = \mathcal{M} - \frac{1}{4}\mathcal{L}^2 - \frac{1}{2}\frac{\partial\mathcal{L}}{\partial z}.$$

One can show that if $\omega > 0$, the upper sign (plus) in solution (6) corresponds to the downward and the lower one (minus) to the upward propagating GWs.

First order correction due to dissipative terms

Assuming that dissipation is weak, we can obtain a first order correction to solution (6). To apply the perturbation theory, we introduce small parameters and reduce the initial set of equations into nondimensional form. Assuming that $k_z \gg 1/H$ (Lindzen, 1981), the initial set of equations (1)-(4) can be written as follows

$$(\varepsilon_u - i\tilde{\omega}^+)\tilde{u} - \frac{1}{\tilde{k}_x}\frac{\partial\tilde{\omega}^+}{\partial\zeta}\tilde{w} + i\tilde{k}_x\tilde{\phi} = 0, \tag{7}$$

$$\frac{d\tilde{\phi}}{d\zeta} = \frac{R\bar{T}}{gH}\tilde{\theta}, \tag{8}$$

$$i\tilde{k}_x\tilde{u} + (\frac{d}{d\zeta} - 1)\tilde{w} = 0, \tag{9}$$

$$(\varepsilon_t - i\tilde{\omega}^+)\tilde{\theta} + \frac{gH}{R\bar{T}}\tilde{N}^2\tilde{w} = 0, \tag{10}$$

where $\varepsilon_u = Dk_z^2/\omega$ and $\varepsilon_t = (Dk_z^2/Pr + \alpha/)\omega$ are small parameters; $\zeta = z/H$ is the nondimensional height; $\tilde{\omega}^+ = \omega^+/\omega$, $\tilde{k}_x = k_x H$, $\tilde{N}^2 = N^2/\omega^2$, g is the acceleration due to gravity; and we introduce the following nondimensional amplitudes of perturbations

$$\begin{aligned}
\tilde{u}(\zeta) &= \frac{\omega u'}{g}\exp[-i(k_x x - \omega t)], \qquad \tilde{w}(\zeta) = \frac{\omega w'}{g}\exp[-i(k_x x - \omega t)], \\
\tilde{\phi}(\zeta) &= \frac{\phi'}{gH}\exp[-i(k_x x - \omega t)], \qquad \tilde{\theta}(\zeta) = \frac{\theta'}{\bar{\theta}}\exp[-i(k_x x - \omega t)].
\end{aligned}$$

Eliminating $\tilde{\theta}$ using (8) and (10), we obtain the perturbed energy equation in terms of the geopotential perturbation

$$(\varepsilon_t - i\tilde{\omega}^+)\frac{d\tilde{\phi}}{d\zeta} + \tilde{N}^2\tilde{w} = 0. \tag{11}$$

Solving (7) with respect to $\tilde{\phi}$ and using the linearized continuity equation (9) to eliminate $\tilde{u}$, we obtain

$$\tilde{\phi} = i\frac{\tilde{\omega}^+}{\tilde{k}_x^2}[(1 + \frac{i\varepsilon_u}{\tilde{\omega}^+})(\frac{d}{d\zeta} - 1) - \frac{1}{\tilde{\omega}^+}\frac{\partial\tilde{\omega}^+}{\partial\zeta}]\tilde{w}. \tag{12}$$

Accounting that $\tilde{k}_z = k_z H \gg 1$ and zero order solution (6), we can rewrite (12) as follows

$$\tilde{\phi} = i\frac{\tilde{\omega}^+}{\tilde{k}_x^2}(\frac{d}{d\zeta} - 1 - \frac{1}{\tilde{\omega}^+}\frac{\partial\tilde{\omega}^+}{\partial\zeta})\tilde{w} + \frac{i\varepsilon_u\tilde{k}_z}{\tilde{k}_x^2}\tilde{w}. \tag{13}$$

The first order solution of (11) with respect to $d\tilde{\phi}/d\zeta$ can be written as follows:

$$\frac{d\tilde{\phi}}{d\zeta} = -i\frac{\tilde{N}^2}{\tilde{\omega}^+}(1 - \frac{i\varepsilon_t}{\tilde{\omega}^+})\tilde{w}. \tag{14}$$

Eliminating $\tilde{\phi}$ in (14) using (13), we obtain

$$(\frac{d^2}{d\zeta^2} - \frac{d}{d\zeta} + \frac{\tilde{N}^2\tilde{k}_x^2}{\tilde{\omega}^{+2}} - \frac{1}{\tilde{\omega}^+}\frac{\partial\tilde{\omega}^+}{\partial\zeta} - \frac{1}{\tilde{\omega}^+}\frac{\partial^2\tilde{\omega}^+}{\partial\zeta^2})\tilde{w} + \frac{\varepsilon_u\tilde{k}_z}{\tilde{\omega}^+}\frac{d\tilde{w}}{d\zeta} - \frac{i\varepsilon_t\tilde{N}^2\tilde{k}_x^2}{\tilde{\omega}^{+3}}\tilde{w} = 0. \tag{15}$$

To obtain the differential equation with real coefficients, we have to rearrange the last term in (15). Accounting that $\tilde{k}_z \approx \tilde{N}\tilde{k}_x/\tilde{\omega}^+ \gg 1$ and using the zero order solution (6), we can write the last term in (15) as follows:

$$-\frac{i\varepsilon_t\tilde{N}^2\tilde{k}_x^2}{\tilde{\omega}^{+3}}\tilde{w} = \frac{\varepsilon_t\tilde{N}^2\tilde{k}_x^2}{\tilde{\omega}^{+3}\tilde{k}_z}\frac{d\tilde{w}}{d\zeta} = \frac{\varepsilon_t\tilde{k}_z}{\tilde{\omega}^+}\frac{d\tilde{w}}{d\zeta}. \tag{16}$$

Comparison between the equations of the first order (15) and zero order (5) with accounting of (16) shows that the dissipative terms only change the expression for $\mathcal{L}$, which in dimensional form can be written as follows:

$$\mathcal{L} = -\frac{1}{H} + \frac{(\varepsilon_u + \varepsilon_t)k_z}{\tilde{\omega}^+} = -\frac{1}{H} + \frac{D(1 + 1/Pr)k_z^3}{\omega^+} + \frac{\alpha k_z}{\omega^+}. \tag{17}$$

Accounting $k_z \approx Nk_x/\omega^+$, we obtain that the dissipative terms in (17) tend to infinity when ω^+ tends to zero, i.e., near a critical level. The perturbation approach is applicable only if these dissipative terms are small in comparison with $1/H$. Usually, an upward propagating GW does not reach the critical level due to breaking or overturning in result of convective instability (see the next paragraph). Nevertheless, in numerical realization we assume that the wave is near a critical level if $\alpha k_z/\omega^+ = O(1/H)$.

Breaking of GWs due to convective instability

Linearized theory is known to give a reasonable representation of even large-amplitude waves observed in the upper atmosphere. It is also used to estimate limits on the maximum amplitudes that such waves can attain (Hodges, 1967, 1969; Lindzen 1968, 1981). Wave overturning (or breaking) due to convective instability occurs if the wave amplitude exceeds a certain limit. In terms of the perturbed potential temperature the breaking condition is $|\partial\theta'/\partial z| \geq \partial\bar{\theta}/\partial z$. This creates a convectively unstable situation and a transition from laminar to turbulent regime. To investigate the situation using the obtained analytical solution, we express this condition in terms of the perturbed vertical velocity. Equation (4) without dissipative terms and taking into account that in equation (6) the exponential term with integral of k_z is the strongest, gives the following approximate relation for breaking conditions

$$|\frac{\partial\theta'}{\partial z}|/\frac{\partial\bar{\theta}}{\partial z} = \frac{k_z|w'|}{\omega^+} \geq 1. \tag{18}$$

Assuming that eddy diffusion limits the further increase in wave amplitude with height, we obtain the saturation condition in the following form

$$\frac{\partial}{\partial z}(\frac{k_z|w'|}{\omega^+}) = 0. \tag{19}$$

Using solution (6), $k_z = k_x N/\omega^+$, and the first order solution for $\mathcal{L}$ (17), we obtain

$$\frac{1}{2H} - \frac{D(1+1/Pr)k_z^3}{2\omega^+} - \frac{\alpha k_z}{2\omega^+} - \frac{3}{2}\frac{1}{\omega^+}\frac{\partial\omega^+}{\partial z} = 0. \tag{20}$$

Solving (20) with respect to the eddy diffusion coefficient D and using $k_z = k_x N/\omega^+$, we obtain (Schoeberl et al., 1983)

$$D = \frac{\omega^{+4}}{k_x^3 N^3(1+1/Pr)}(\frac{1}{H} - \frac{\alpha k_z}{\omega^+} - 3\frac{1}{\omega^+}\frac{\partial\omega^+}{\partial z}). \tag{21}$$

Mean flow acceleration due to dissipation and/or breaking of GWs

Under breaking conditions GWs accelerate the mean flow due to vertical divergence of the horizontal momentum flux. Usually, following the suggestions by Lindzen (1981), this forcing per unit mass is calculated using the obtained expressions for D (21) and $\mathcal{L}$ (17) and assuming that GWs are under breaking condition everywhere above the first breaking level (Schoeberl et al., 1983; Holton and Zhu, 1984; Hunt, 1986; Jakobs et al., 1986). However, the background wind can substantially influence the propagation conditions of GWs (Pogoreltsev and Pertsev, 1996) and we have to expect the wave overturning only in some layers where the breaking condition is satisfied (Akmaev, 2001). Especially this is important when the "mean" flow includes large-scale atmospheric waves with a short vertical wavelength (for instance, at low latitudes in the MLT region, where the diurnal tide and sometimes Kelvin waves have substantial amplitudes). To take into account such possibility, we consider the divergence of the horizontal momentum flux. The forcing per unit mass due to this divergence can be written using equation (3) and solution (6) as follows

$$a = -\frac{1}{\rho}\frac{\partial}{\partial z}(\rho\overline{u'w'}) = -\frac{1}{\rho}\frac{\partial}{\partial z}(\rho\frac{k_z\overline{w'^2}}{k_x}) = \frac{|w'|^2 k_z}{2k_x}(\mathcal{L} + \frac{1}{H}), \tag{22}$$

accounting being taken that $w'^2 = 0.5|w'|^2$. Equation (22) shows that without dissipation ($\mathcal{L} = -1/H$) the GWs do not accelerate the mean flow. Using the first order solution for $\mathcal{L}$ (17), we obtain

$$a = \frac{|w'|^2 k_z^2}{2k_x\omega^+}[D(1+1/Pr)k_z^2 + \alpha]. \tag{23}$$

Substituting $|w'|_b = \omega^+/k_z$ (amplitude of the vertical velocity perturbation at breaking level) and eddy diffusion coefficient D (21) in (23), we obtain the explicit expression for the forcing per unit mass, which usually has been used to calculate the GW drag in general circulation models (Schoeberl et al., 1983; Holton and Zhu, 1984; Hunt, 1986; Jakobs et al., 1986) with the Lindzen (1981) parameterisation

$$a = \frac{\omega^+}{2k_x}[\frac{\omega^{+2}}{k_x N}(\frac{1}{H} - \frac{\alpha k_z}{\omega^+} - 3\frac{1}{\omega^+}\frac{\partial\omega^+}{\partial z}) + \alpha] \approx \frac{\omega^{+3}}{2k_x^2 N}(\frac{1}{H} - 3\frac{1}{\omega^+}\frac{\partial\omega^+}{\partial z}). \tag{24}$$

However, as is noted above, this parameterisation assumes that GWs are under breaking condition everywhere above the first breaking level. To apply the Lindzen-type parameterisation of the GW drag to background conditions with a strong variability of zonal and meridional winds with altitude, we follow the suggestions by Akmaev (2001). Stepping up from a given height level z, it is sufficient to calculate $|w'(z+\Delta z)|$ using the WKB solution (6) with $\mathcal{L}$ taking into account some background dissipation (radiative damping in our case). The second integral in the right-hand part of (6) can be estimated using the simplest quadrature formula (Gavrilov, 1990). $|w'(z+\Delta z)|$ is next compared with the breaking value $|w'|_b = \omega^+/k_z$. If $|w'(z+\Delta z)|$ exceeds $|w'|_b$, then it is reset to $|w'|_b$, the GW assumed to break between z and $z+\Delta z$, and the forcing per unit mass (22) is calculated by finite differences

$$\begin{aligned} a(z+\Delta z/2) &= \frac{1}{2k_x}\Big[\frac{k_z(z+\Delta z)|w'(z+\Delta z)|^2 + k_z(z)|w'(z)|^2}{2H} \\ &- \frac{k_z(z+\Delta z)|w'(z+\Delta z)|^2 - k_z(z)|w'(z)|^2}{\Delta z}\Big]. \end{aligned} \tag{25}$$

Otherwise, the wave is assumed to propagate free of breaking and acceleration of the mean flow is conditioned only by radiative damping of GWs. It should be noted that in practice the GW levels are situated between the levels of the COMMA-LIM model, and accelerations in zonal and meridional directions are calculated as follows

$$a_\lambda = a\cos\vartheta, \qquad a_\vartheta = a\sin\vartheta,$$

where ϑ is the azimuth of GW propagation.

Using $|w'(z_k)|$, we can estimate more correctly the eddy diffusion coefficient. One can obtain from solution (6) the following relation:

$$\frac{\partial}{\partial z}\ln(k_z^{1/2}|w'|) = -\mathcal{L}/2. \tag{26}$$

Substituting $\mathcal{L}$ (17) into (26) and solving the obtained equation with respect to D, we obtain

$$D = \frac{\omega^+}{k_z^3(1+1/Pr)}\Big[\frac{1}{H} - \frac{\alpha k_z}{\omega^+} - 2\frac{\partial}{\partial z}\ln(k_z^{1/2}|w'|)\Big], \tag{27}$$

which will be used to estimate the cooling/heating contribution of the GWs. To calculate $D(z_k+\Delta z/2)$, i.e., at the COMMA-LIM levels, the ω^+ and k_z averaged over GW levels z_k are used, and the last term in (27) is calculated by finite differences.

Heating/cooling of the atmosphere by GWs

Accounting that in log-pressure coordinates $\bar{T} = \bar{\theta}\exp(-\kappa z/H)$, the thermodynamic equation can be written in terms of the background temperature (Schoeberl et al., 1983)

$$\frac{\partial\bar{T}}{\partial t} + \overline{\mathbf{V}}\cdot\nabla\bar{T} + \bar{w}\frac{\kappa\bar{T}}{H} = -\frac{\bar{T}}{\bar{\theta}}\frac{1}{\rho}\frac{\partial}{\partial z}(\rho\overline{w'\theta'}) + \frac{\bar{T}}{\bar{\theta}}\frac{1}{\rho c_p}\frac{\partial}{\partial z}(\rho c_p\frac{D}{Pr}\frac{\partial\bar{\theta}}{\partial z}) + \bar{Q} - \bar{C}, \tag{28}$$

where $\bar{Q}$ and $\bar{C}$ are the mean heating and cooling per unit mass, respectively. Later the overbars denoting the background state will be omitted. The first term in the right-hand side of equation (28) describes the heating/cooling effects due to GW dissipation.

Accounting that $\theta'/\theta = T'/T$, we obtain in terms of the heat flux:

$$-\frac{T}{\theta\rho}\frac{\partial}{\partial z}(\rho\overline{w'\theta'}) = -\frac{1}{\rho}\frac{\partial}{\partial z}(\rho\overline{w'T'}) - \frac{\kappa}{H}\overline{w'T'}. \tag{29}$$

Using the zero order solution for GWs and equation (4) we can obtain the following expression:

$$\frac{\overline{w'\theta'}}{\theta} = \frac{\overline{w'T'}}{T} = -(\alpha + Dk_z^2/Pr)(\frac{1}{\theta}\frac{\partial\theta}{\partial z})^{-1}\frac{\overline{\theta'^2}}{\theta^2} = -\frac{(\alpha + Dk_z^2/Pr)}{2}(\frac{1}{\theta}\frac{\partial\theta}{\partial z})^{-1}\frac{|\theta'^2|}{\theta^2}. \tag{30}$$

Taking into account the polarisation relation between θ' and w' [zero order solution of equation (4)], we obtain

$$(\frac{1}{\theta}\frac{\partial\theta}{\partial z})^{-1}\frac{|\theta'^2|}{\theta^2} = \frac{1}{\omega^{+2}}\frac{1}{\theta}\frac{\partial\theta}{\partial z}|w'|^2, \tag{31}$$

and the heat flux in terms of the vertical velocity perturbation can be written as follows

$$\overline{w'T'} = -\frac{HN^2(\alpha + Dk_z^2/Pr)}{2R\omega^{+2}}|w'|^2 \approx -\frac{Hk_z^2(\alpha + Dk_z^2/Pr)}{2Rk_x^2}|w'|^2, \tag{32}$$

accounting being taken that

$$\frac{1}{\theta}\frac{\partial\theta}{\partial z} = \frac{H}{RT}N^2.$$

The dissipative GW deposits energy in the atmosphere, and in the presence of a wind shear the energy conservation equation for GW can be written as follows (Plumb, 1983):

$$\frac{\partial E}{\partial t} + \nabla\cdot\mathbf{F} = \frac{\rho}{k_x}\frac{\partial\omega^+}{\partial z}\overline{u'w'} - S_{GW}, \tag{33}$$

where

$$\begin{aligned} E &= \frac{\rho}{2}[\overline{u'^2} + N^2(\frac{\partial\theta}{\partial z})^{-2}\overline{\theta'^2}], \\ \mathbf{F} &= \rho\overline{\mathbf{V}'\phi'} - \mathbf{i}_z\rho D[\overline{u'\frac{\partial u'}{\partial z}} + \frac{N^2}{Pr}(\frac{\partial\theta}{\partial z})^{-2}\overline{\theta'\frac{\partial\theta'}{\partial z}}], \end{aligned}$$

and $\mathbf{i}_z$ is the unit vector along the vertical coordinate. The first term in the right-hand side of (33) is the conversion of GW kinetic energy to the kinetic energy of the mean state. The nonconservative sink term S_{GW} describes the loss of the GW energy due to dissipation and can be written as follows

$$S_{GW} = N^2(\frac{\partial\theta}{\partial z})^{-2}[\rho\frac{D}{Pr}\overline{(\frac{\partial\theta'}{\partial z})^2} + \alpha\rho\overline{\theta'^2}] + \rho D\overline{(\frac{\partial u'}{\partial z})^2}. \tag{34}$$

Using polarisation relations of GWs [equations (3)-(4) without dissipative terms] and taking into account that

$$k_z \gg 1/H, \qquad \overline{(\frac{\partial\theta'}{\partial z})^2} = 0.5\mathrm{Re}[\frac{\partial\theta'}{\partial z}(\frac{\partial\theta'}{\partial z})^*] \approx 0.5k_z^2|\theta'|^2,$$

where * denotes a complex conjugate value, we obtain

$$S_{GW} = \frac{\rho}{2}[\frac{N^2}{\omega^{+2}}(\alpha + \frac{Dk_z^2}{Pr}) + \frac{Dk_z^4}{k_x^2}]|w'|^2 \approx \frac{\rho N^2[\alpha + Dk_z^2(1/Pr + 1)]}{2\omega^{+2}}|w'|^2, \qquad (35)$$

or in terms of the heat flux [see (32)]

$$S_{GW}/\rho c_p = -(1 + \frac{D}{\alpha + Dk_z^2/Pr})\frac{\kappa}{H}\overline{w'T'}. \qquad (36)$$

Comparison between (36) and (29) shows that the last term in the right-hand side of (29) can be interpreted as the local heating rate due to conversion of the potential energy provided by GW dissipation into heat [see also (34) and (35)]. This term appears in (28) explicitely. The second term in the right-hand side of (36) describes the mechanical energy provided by GW dissipation. Some part of this energy is lost through production of turbulence and/or other waves that remove energy from the region considered. The remaining mechanical energy will be converted into heat (Schoeberl et al., 1983; Medvedev and Klaassen, 2002), and we have to introduce the corresponding heating term into the right-hand side of (28). Finally, the total heating rate due to GW dissipation can be written as follows:

$$Q_{GW} = -\frac{1}{\rho}\frac{\partial}{\partial z}(\rho\overline{w'T'}) - (1 + e_{wh}\frac{D}{\alpha + Dk_z^2/Pr})\frac{\kappa}{H}\overline{w'T'}, \qquad (37)$$

where $e_{wh} \leq 1$ is an efficiency of the mechanical energy conversion into heat. It should be noted that without dissipation $\overline{w'\theta'} = \overline{w'T'} = 0$ [see (32)] and GWs do not interact with the mean state.

Gravity waves are given at each horizontal gridpoint in the troposphere (at an altitude of about 7 km with 6 different phase speeds from 5 to 30 m/s and 8 azimuth angles of propagation from 0° to 315°. The amplitudes of the perturbed vertical velocity are choosen equal to 0.75 cm/s and horizontal wavelenghts are fixed at 300 km. For the Newtonian cooling coefficient we use the parameterisation of radiative damping rate given by Zhu (1993).

1.2 Solar Tides and Planetary Waves

Solar tides are generated in the model directly by absorption of radiation (see next section). A set of stationary (with zonal wave number m=1, 2) and travelling (the Rossby normal-mode and Kelvin waves) planetary waves can now be introduced into COMMA-LIM at the lower boundary. For stationary planetary waves for each month 11-year averaged monthly mean UKMO assimilated data are included in the geopotential height field at 1000 hPa. This gives really different lower boundary conditions for each season and is one of the main reasons for different summer and winter pictures in each hemisphere which otherwise will be approximately mirrored. To include travelling Rossby and Kelvin waves, the corresponding Hough functions are calculated (Swarztrauber and Kasahara, 1985) and these waves are added to the geopotential height at the lower

boundary after switching on the forcing.

Heating of the atmosphere due to dissipation of the resolved motions
The resolved waves (solar tides and planetary waves) and mean flow deposite a mechanical energy in the atmosphere due to dissipation by molecular and turbulent viscosity, ion drag and Rayleigh friction. A part of this energy is lost through radiation and/or generation of other waves. The remaining energy has to be converted into heat. The viscous term in the energy balance equation can be separated into the "flux" and "dissipative" (always negative) parts. The loss of energy ("dissipative" part) can be written as follows

$$\varepsilon_v = -\frac{\mu}{\rho}(\frac{H}{H_T})^2[(\frac{\partial u}{\partial z})^2 + (\frac{\partial v}{\partial z})^2], \tag{38}$$

where the dynamic viscosity $\mu = \mu_m + \rho\nu_e$, μ_m is the dynamic molecular viscosity, and ν_e is the kinematic eddy viscosity. The molecular viscosity coefficient μ_m is calculated using the thermal conduction coefficient K_m by Eucken formula derived from kinetic theory (Forbes and Garrett, 1979)

$$\mu_m = \frac{K_m}{0.25(9c_p - 5c_v)}, \tag{39}$$

where c_v is the specific heat at constant volume.

The losses of energy due to ion drag and Rayleigh friction can be presented in the following form

$$\varepsilon_{fr} = -\beta_{r\lambda}u^2 - \beta_{r\varphi}v^2, \tag{40}$$

where $\beta_{r\lambda}$ and $\beta_{r\varphi}$ are the combined ion drag and Rayleigh friction coefficients in the zonal and meridional momentum equation, respectively.
The most part of this mechanical energy has to be converted into heat and we have to include an additional heating term in the thermodynamic equation:

$$Q_M = -e_M(\varepsilon_v + \varepsilon_{fr})/c_p, \tag{41}$$

where e_M is the efficiency of the mechanical energy conversion into heat for the resolved waves and the mean flow. In the present study $e_M = 1$ has been used.

1.3 Cooling/heating of the atmosphere by turbulence and molecular thermal conduction

Accounting the temperature stratification of the atmosphere, the second term in the right-hand side of the thermodynamic equation (28) can be written as follows

$$\frac{T}{\theta}\frac{H}{H_T}\frac{1}{\rho c_p}\frac{\partial}{\partial z}(\rho c_p\frac{D}{Pr}\frac{H}{H_T}\frac{\partial\theta}{\partial z}) = \frac{H}{H_T}\frac{1}{\rho c_p}\frac{\partial}{\partial z}[\rho K_h(\frac{H}{H_T}\frac{\partial T}{\partial z} + \frac{g}{c_p})] + \frac{\kappa K_h}{c_p H_T}(\frac{H}{H_T}\frac{\partial T}{\partial z} + \frac{g}{c_p}), \tag{42}$$

where $H = const$ and $H_T(z) = RT/g$ is the scale height for the atmosphere with a stratification of the temperature; $K_h = c_p D/Pr$ is the coefficient of turbulent

thermal conduction. It should be noted that there are several sources of turbulence, for instance, shear instability of the mean flow, breaking of solar tides and planetary waves. It means that in general $K_h \neq c_p D/Pr$, where D is the eddy diffusion coefficient conditioned by the GW breaking. In practice we suggest to use the eddy diffusion coefficient D (27) only to calculate the heating/cooling rate due to GW breaking, but in the thermodynamic equation to use $K_h(z) = c_p \nu_e(z)/Pr$, where the kinematic eddy viscosity $\nu_e(z)$ is given by an analytical formula. We assume that turbulence in the middle atmosphere is generated within relatively thin layers, and the effective eddy heat exchange is weaker than eddy transport of momentum, i.e., $Pr > 1$ (Coy and Fritts, 1988; Gavrilov and Yudin, 1992). In the present study we accept $Pr = 3$.

The heating term Q in (28) contains also the heating per unit mass due to dissipation of the turbulent energy ε_d/c_p (Izakov, 1978), and we can write the thermodynamic equation (28) in the following form

$$\frac{\partial T}{\partial t} + \mathbf{V} \cdot \nabla T + w\frac{\kappa T}{H} = -\frac{H}{H_T}\frac{1}{\rho c_p}\frac{\partial q_t}{\partial z} + \frac{\varepsilon_b + \varepsilon_d}{c_p} + Q - C, \tag{43}$$

where the turbulent flux of heat q_t and work against the buoyancy force ε_b are written as follows:

$$q_t = -\rho K_h\left(\frac{H}{H_T}\frac{\partial T}{\partial z} + \frac{g}{c_p}\right), \qquad \varepsilon_b = \frac{g}{T}\frac{K_h}{c_p}\left(\frac{H}{H_T}\frac{\partial T}{\partial z} + \frac{g}{c_p}\right).$$

To estimate the role of the heating due to dissipation of the turbulent energy ε_d, we consider the balance equation of the turbulent energy (Monin and Yaglom, 1975)

$$\frac{de_t}{dt} = \varepsilon_s - \varepsilon_b - \varepsilon_d = (1 - Ri_f)\varepsilon_s - \varepsilon_d, \tag{44}$$

where e_t is the turbulent energy per unit mass, ε_s is the source of turbulent energy due to shear instability of the mean flow, and $Ri_f = \varepsilon_b/\varepsilon_s$ is the dynamical (or flux) Richardson number (see Izakov, 1978). Under steady-state conditions $de_t/dt = 0$ we obtain

$$\varepsilon_d = \frac{1 - Ri_{fc}}{Ri_{fc}}\varepsilon_b, \tag{45}$$

where the critical flux Richardson number $Ri_{fc} = 1 - \varepsilon_d/\varepsilon_s$. In this case the thermodynamic equation can be written as follows:

$$\frac{\partial T}{\partial t} + \mathbf{V} \cdot \nabla T + w\frac{\kappa T}{H} = -\frac{H}{H_T}\frac{1}{\rho c_p}\frac{\partial q_t}{\partial z} + \frac{\varepsilon_b}{c_p Ri_{fc}} + Q - C. \tag{46}$$

Under stable stratification the divergence of the turbulent heat flux produces the cooling of the atmosphere, and equation (42) shows that the relative role of cooling/heating due to turbulence depends on the value of the critical flux Richardson number. It seems that introducing Ri_{fc} is simply some kind of manipulation, nevertheless, it is useful to use this number as a free tunable parameter in a numerical simulation. Measurements show that for the Earth's thermosphere $0.2 \leq Ri_{fc} \leq 0.6$ (Izakov, 1978).

Following Gavrilov and Shved (1975), Ebel (1984) proposed to include into the turbulence energy equation the additional source ε_w and sink ε_c terms, which are conditioned by production of turbulence due to GW breaking and conversion of turbulent energy into the energy of regular motions (for instance, the generation of other waves). In this case we can also introduce the generalized Richardson number as $Ri_f^* = \varepsilon_b/(\varepsilon_s + \varepsilon_w - \varepsilon_c)$ and use Ri_{fc}^* obtained from steady-state conditions instead of Ri_{fc}. This suggestion assumes that the loss of GW energy due to dissipation and/or breaking will be converted into heat through the generation of turbulent motions and we have to put the efficiency of GW heating $e_{wh} = 0$. However, in practice of numerical simulation, to investigate separately the heating/cooling effects of GW breaking and turbulence, it is more useful to have two tunable parameters e_{wh} and Ri_{fc}. It should be noted that in general these parameters are not independent (decrease in e_{wh} leads to a decrease in Ri_{fc}), but this dependence is not well defined because there are different sources of atmospheric turbulence (shear instability, GW breaking, breaking of resolved waves and so on), and a part of the turbulent energy can be converted into the energy of mean or wave motions. In the present simulations $e_{wh} = 0.3$ and $Ri_{fc} = 0.6$ have been used.

In the thermosphere the molecular thermal conduction plays an important role, and we have to replace q_t in (42) by $q = q_t + q_m$, where the molecular flux of heat q_m can be presented as follows:

$$q_m = -K_m \frac{H}{H_T} \frac{\partial T}{\partial z},$$

K_m is the molecular thermal conduction coefficient, which is calculated by a semiempirical formula (Forbes and Garrett, 1979) $K_m = K_{m0} T^{2/3}/M$, where $K_{m0} = 0.015$ $JK^{-1}\mathrm{m}^{-1}\mathrm{s}^{-1}$ and M is the mean molecular weight in atomic mass units.

1.4 Parameterisation of the horizontal turbulent diffusion

To smooth the subgrid-scale motions, instead of the Shapiro-Filter we now use the parameterisation of the horizontal turbulent diffusion suggested by Marchuk et al. (1984). In the simplest form the terms describing horizontal diffusion in the zonal and meridional momentum equations can be written as follows:

$$F_u^H = \frac{K_H}{a^2 \cos^2\varphi}\left[\frac{\partial^2 u}{\partial^2 \lambda} + \frac{\partial}{\partial \varphi}\cos^3\varphi \frac{\partial}{\partial \varphi}\left(\frac{u}{\cos\varphi}\right) - 2\sin\varphi \frac{\partial v}{\partial \lambda}\right], \tag{47}$$

$$F_v^H = \frac{K_H}{a^2 \cos^2\varphi}\left[\frac{\partial^2 v}{\partial^2 \lambda} + \frac{\partial}{\partial \varphi}\cos^3\varphi \frac{\partial}{\partial \varphi}\left(\frac{v}{\cos\varphi}\right) + 2\sin\varphi \frac{\partial u}{\partial \lambda}\right], \tag{48}$$

where K_H is the coefficient of the horizontal diffusion. The corresponding term in the energy equation is the following:

$$F_T^H = \frac{K_H}{a^2 \cos^2\varphi}\left[\frac{\partial^2 T}{\partial^2 \lambda} + \cos\varphi \frac{\partial}{\partial \varphi}\left(\cos\varphi \frac{\partial T}{\partial \varphi}\right)\right]. \tag{49}$$

In our simulation we use the height dependent coefficient of the horizontal diffusion

$$K_H(z) = [1.25 + 0.75 \tanh(\frac{z - z_0}{20})]10^6 \text{ m}^2\text{s}^{-1}, \tag{50}$$

where z is the altitude in kilometers and z_0=40 or 60 km (strong or weak coefficient of the horizontal diffusion in the stratosphere).

Additionally, to suppress the motions with small (unresolved) vertical scales, we introduce a weak vertical bi-harmonic diffusion in the model, which practically does not influence the considered large-scale waves and mean flow.

1.5 Ion drag, Lorentz deflection, and Rayleigh friction terms

In the lower thermosphere (dynamo-region of the ionosphere) interaction between the ionised and neutral components can substantially influence the large-scale neutral gas motions. To take into account this interaction, we have to include the electromagnetic force $c^{-1}[\mathbf{j} \times \mathbf{B}]$ into the momentum equation, where c is the speed of light, $\mathbf{B}$ is the geomagnetic field, and electric current density $\mathbf{j}$ can be presented as follows:

$$\mathbf{j} = \sigma_0(\mathbf{E}' \cdot \mathbf{B})\mathbf{B}/B_0^2 + \sigma_1 \mathbf{B} \times \mathbf{E}' \times \mathbf{B}/B_0^2 + \sigma_2 \mathbf{B} \times \mathbf{E}'/B_0, \tag{51}$$

where $\mathbf{E}' = \mathbf{E} + c^{-1}[\mathbf{V} \times \mathbf{B}]$; σ_0, σ_1, and σ_2 are parallel, Pedersen, and Hall conductivities, respectively. Assuming $\mathbf{E}$=0 (consideration of the electrostatic electric field is out of scope of the present paper) and using the geomagnetic field in the form of magnetic dipole $\mathbf{B} = B_0\{0, \cos\varphi/(1+3\sin^2\varphi)^{1/2}, -2\sin\varphi/(1+3\sin^2\varphi)^{1/2}\}$, we obtain the ion drag and Lorentz deflection terms, which can be presented as additional Rayleigh friction coefficients in the zonal and meridional momentum equations and correction to the Coriolis term, respectively

$$\beta_{r\lambda} = \beta_r + \frac{\sigma_1 B_0^2}{\rho c^2}, \qquad \beta_{r\varphi} = \beta_r + \frac{\sigma_1 B_z^2}{\rho c^2}, \tag{52}$$

and

$$2\Omega \sin\varphi \quad -> \quad (2\Omega - \frac{\sigma_2 B_0 B_z}{\rho c^2}) \sin\varphi. \tag{53}$$

Daily averaged profiles of Pedersen and Hall conductivities are calculated as averaged over low latitudes ($-45^0 \le \varphi \le 45^0$) using empirical models of the thermosphere and ionosphere and standard expressions for collision frequencies (Pogoreltsev, 1996). The calculated profiles of ion drag and Lorentz deflection terms are interpolated to pressure levels using the geopotential height.

The background Rayleigh friction coefficient β_r is introduced to parameterise the loss of energy due to nonlinear interaction of the mean flow and resolved waves with other waves, which are not taken into consideration. The role of the nonlinear processes increases with altitude (McLandress, 2002), and we use the following analytical formula to account this effect

$$\beta_r(z) = [1.25 + 0.75 \tanh(\frac{z - z_0}{20})]10^{-6} \text{ s}^{-1}, \tag{54}$$

where z and z_0 are defined as above (and here it means strong or weak coefficient of the Rayleigh friction in the stratosphere).

2 Heating due to absorption of solar radiation

Heating of the most important gases as water vapor, carbon dioxide, ozone and oxygen is considered. Water vapor is the most important absorber in the troposphere. Ozone clearly dominates stratospheric heating and molecular oxygen becomes more and more important between 60 and 120 km. We prescribe the water vapor content in an analytic profile symmetric to the equator. Carbon dioxide is assumed to be equally distributed up to $\sim$ 80 km and decreasing above, the volume mixing ratio is set to 360 $ppmV$; but CO_2 gives the most substantial contribution to heat in the troposphere because its absorption is strongly dependent on the pressure ratio. Ozone data are used from the Berlin climatology (Fortuin and Langematz, 1994), atomic and molecular oxygen are given as climatological globally averaged profiles of the mixing ratio.

The original Strobel-parameterisation as described in Lange (2001) has been extended and improved taking into account several new investigations on this topic. Ozone heating in the Chappius, Herzberg and Huggins bands has been improved due to Rickaby and Shine (1989). These bands are splitted into several sections in order to increase the accuracy of the calculation. Now, also the Lyman-α band is included, which is important because of its strong variation during the solar cycle. O_2 heating in the Hartley, Schumann-Runge bands and the Schumann-Runge Continuum is retained following Strobel (1978) but includes new efficiency coefficients according to Mlynzak and Solomon (1993). Processes of chemical heating due to recombination reactions of O_2 and O_3 are added to the heating routine according Riese and Offermann (1994).

Heating due to absorption of H_2O and CO_2 is newly adjusted according to Liou (1992) as will be pointed out below. Rayleigh scattering and surface reflection are taken into account for heating of H_2O, because this is the most important absorber in the troposphere.

2.1 Transfer of broadband solar flux in the atmosphere

First consider a nonscattering atmosphere. The direct downward solar flux at level τ is given by the exponential attenuation of the effective solar flux at the top of the atmosphere (TOA) $\mu_0 F_{\lambda\infty}$. Thus

$$F^{-}_{dir}(\tau) = \mu_0 F_{\lambda\infty} exp^{-\tau/\mu_0}, \tag{55}$$

where $\mu_0 = \cos\vartheta_0$, ϑ_0 denotes the solar zenit angle, and for monochromatic direct solar flux, the total direct downward solar flux can be written as

$$F_s(z) = \int_0^\infty \mu_0 F_{\lambda\infty} \exp(-\frac{k_\lambda u(z)}{\mu_0}) d\lambda, \tag{56}$$

where $k_\lambda u(z)$ represents the optical depth, k_λ is the absorption coefficient, and the absorbing gaseous path length is defined by

$$u(z) = \int_z^{z_\infty} \rho_a(z')dz\prime, \tag{57}$$

where ρ_a denotes the density of the absorbing gas and z_∞ denotes the height at TOA. The total solar flux at TOA can be written as follows

$$S = \int_0^\infty F_{\lambda\infty} d\lambda, \tag{58}$$

and monochromatic absorptance may be expressed by

$$A_\lambda(u/\mu_0) = 1 - \exp(-k_\lambda u/\mu_0). \tag{59}$$

We may define broadband solar absorptance as follows (Liou, 1992):

$$A(z) = \frac{1}{S}\int_0^\infty F_{\lambda\infty} A_\lambda(u/\mu_0) d\lambda, \tag{60}$$

and equation (56) can be rewritten in the form

$$F_s(z) = \mu_0 S[1 - A(z)]. \tag{61}$$

Broadband solar absorptance may be rewritten in terms of spectral absorptance A_i in the form

$$A(z) = \int_0^\infty A_\lambda(u/\mu_0) w_\lambda d\lambda \approx \sum_i A_i(u/\mu_0) w_i \Delta\lambda_i, \tag{62}$$

where $w_\lambda = F_{\lambda\infty}/S$.

For large values of total absorption, the empirical expression for the mean spectral absorptivity can be written as follows (Liou and Sasamory, 1975):

$$\bar{A}_i = A_i \Delta\lambda_i = \frac{1}{\Delta\nu_i}[C_i + D_i \log_{10}(u p^{\eta_i}/\mu_0 + \chi_{0i})], \tag{63}$$

or in terms of the reduced pressure $\tilde{p}$ (Liou, 1992)

$$\bar{A}_i = \frac{1}{\Delta\nu_i}[C_i + D_i \log_{10}(\tilde{p}/\mu_0 + \chi_{0i})], \tag{64}$$

where

$$\tilde{p}_i = \int_0^u p^{\eta_i} du = \int_z^{z_\infty} \rho_a p^{\eta_i} dz'. \tag{65}$$

The heating rate can be written as follows (Liou, 1992):

$$(\frac{\partial T}{\partial t})_s = -\frac{\mu_0 S}{\rho c_p}\sum_i w_i \frac{d\bar{A}_i(u/\mu_0)}{dz} = \frac{\mu_0 S \rho_a}{\rho c_p}\sum_i w_i \frac{d\bar{A}_i(u/\mu_0)}{du}, \tag{66}$$

where

$$\frac{d\bar{A}_i(u/\mu_0)}{du} = \frac{\log_{10} e}{\mu_0}\sum_i \frac{D_i}{\Delta\nu_i}(\tilde{p}_i/\mu_0 + \chi_{0i})^{-1}\frac{d\tilde{p}_i}{du}, \tag{67}$$

and

$$\frac{d\tilde{p}_i}{du} = p^{\eta_i}. \tag{68}$$

Finally, taking into account Rayleigh scattering and surface reflection (Liou, 1992), we obtain

$$(\frac{\partial T}{\partial t})_s = \frac{S\rho_a \log_{10} e}{\rho c_p} \sum_i \frac{w_i D_i}{\Delta\nu_i} \{ \frac{p^{\eta_i}}{\tilde{p}_i/\mu_0 + \chi_{0i}} + \frac{\mu_0 r(\mu_0)}{\bar{\mu}} [1 - A(z_b)] \frac{p^{\eta_i}}{\tilde{p}_{b_i}/\bar{\mu} + \chi_{0i}} \}, \tag{69}$$

where $r(\mu_0)$ is the combined reflection due to the Rayleigh layer and the surface, $1/\bar{\mu}$ is the diffusivity factor, $z_b = 0$ for water vapor absorption, and

$$\tilde{p}_{b_i} = \int_{z_b}^{z} \rho_a p^{\eta_i} dz'. \tag{70}$$

3 Results and Discussion

Now, we will dicuss the results COMMA-LIM is capable of producing. Figures 1 to 8 show latitude-height cross sections of monthly mean temperature and wind fields, tides and stationary planetary wave with wavenumber 1 for all four seasons. Calculations were done for January, April, July and October in order to obtain the stabilized climatologies which develope just after solstice or equinox, respectively. Please note, that we used here a moderate dissipation in the stratosphere with $z_0 = 50\ km$ (see equation (50) and (54)). Further, no travelling planetary waves are excited and only the stationary planetary wave with wavenumber 1 is forced at lower boundary.

Temperature field
First, note the temperature fields (top panels of Figures 1 to 4). Observed features of the atmosphere are (Scaife et al., 2000): a cold equatorial tropopause about/below 210 K, a cold winter stratosphere together with a raised winter stratopause, a strongly heated stratosphere/stratopause at the summer hemisphere due to absorption by ozone and above a very cold summer mesopause region with temperatures up to 130 K. While the temperature maximum at the summer stratopause and the minimum in the polar winter stratosphere derived from radiation processes the other extremes develope through the meridional circulation and eddy motions in the middle atmosphere. One can see that the model matches this features well. In January and July, the summer mesopause temperatures are below 150 K. It fits not excatly the 130 K finding because there is still a lack of knowledge to what amount gravity waves, tides and planetary waves act to cool the mesopause region. For April and October one can see, that the stratopause looks very similar to that of the following solstice conditions, whereas the mesopause region shows a transitional picture.

Wind fields
Again, several properties have to be mentioned to understand the climatological pictures. At solstice, the circulation consists of rising air near the summer pole, a meridional drift to the winter hemisphere, and sinking near the winter pole. The Coriolis torque excerted by this meridional drift tends to generate mean zonal westerlies in the winter hemisphere and easterlies in the summer hemisphere that are in

approximate geostrophic balance with the meridional pressure gradient. At equinoxes the maximum heating at equator leads to rising air there and poleward drift in both spring and autumn hemispheres. The Coriolis torque thus generates weak zonal mean westerlies in both hemispheres. In the troposphere, easterly jets arise in the subtropical regions - the trade winds - and a westerly jet arises at midlatitudes. In the mesopause region the momentum deposition of breaking gravity waves leads to a zonal wind reversal.

The climatological values for the zonal and meridional winds can be easily recognised. For the troposphere one has to take into account that we only have four layers to describe it and no hydrological cycle. The troposphere therefore acts as a lower boundary and we have only very rough dynamical conditions.

We compare our zonal winds with wind measurements from the High Resolution Doppler Imager (HRDI) which were combined with results from the UK Met. Office stratospheric data asssimilation system, see also Swinbank and Ortland (paper at UARS-website). They published monthly mean values from April 1992 to March 1993.

Beginning with the troposphere, one can see the easterly jets appear only at solstice conditions and only in the summer tropical region. The westerly jets in both hemispheres with maxima are at about 40 ° North or South. The absolute values of the westward winds in the winterhemisphere are slightly weak compared with the climatological values. But one can see the asymmetric seasonal behaviour that is conditioned by the topography of the earth. We obtain this feature mainly due to seasonally different stationary planetary waves with wavenumber 1 (SPW1).

In the stratophere and mesosphere the easterly and westerly jets dominate in each summer (winter) side in July and January, respectively. In a good agreement with this wind data is the winter jet for July and January, which is stronger in July and weaker in January. However, the summer (easterly) jet in COMMA-LIM is about 20 $m\ s^{-1}$ weaker and has only one maximum instead of two as observed. Several things are assumed to be responsible for this difference: first, there is no latitudinal variation of GW's which provide acceleration on the mean flow due to their breaking; second, no planetary waves besides the SPW1 are included. Another reason can be the medium scale variability in ozon (and heating rate) which is not presented in the climatological fields. In the transition time (April and October) we have westerly jets on both hemispheres where the autumn jet is (two times) stronger than the spring one. The results for April match better than these for October. The mesopause region is characterized by the zonal wind reverse due to the momentum deposition of breaking gravity waves. The measurements show a weaker reverse of the jets on winter hemispheres which can be driven by decreased gravity wave activity. COMMA-LIM has until now included no seasonal dependence of GW activivy; this is a seperate work. Therefore no difference in the strenght of the reversal jets can bee seen in our July and January Figures. The meridional winds show very nice the circulation for solstices and equinoxes as it is explained above.

Tides and the stationary planetary wave

Our figures 5 to 8 show the diurnal tide at the top, the semidiurnal tide at the middle - both as amplitudes in the zonal wind - and the SPW1 in geopotential height at bottom

for all four months. It can bee seen that the diurnal tide has a seasonal variation which is also observed (McLandress, 2002): it is stronger at equinox and weaker at solstice. The maxima appear around 30 ° North and South at altitudes between 90 and 100 km. This coincides with measurements derived from HRDI data for $1992 - 1993$, see also Khattatov et al. (1997). The absolute values are different, COMMA-LIM shows approximately 10 m/s higher amplitudes than the HRDI data. But taken into account that the control runs are done without any travelling planetary wave these results cannot be totally identical. The maxima of semidiurnal tides prevail at higher latitudes and have higher values in winter than in summer as can be clearly seen in the figures. Comparisons with results obtained by assimilating ground based data into a model (Portnyagin and Solovjova, 1998) confirm the locations of our maximum amplitudes.

Considering the stationary planetary wave one recognises that SPW1 is strongest in winter, espescially in the northern hemisphere winter. This is in good agreement with analyses from Labitzke (1985).

Conclusion

We introduced in COMMA-LIM a new gravity wave parameterisation and connected processes as heating and cooling of the atmosphere by GW. Further, the included planetary waves are also considered as sources of mechanical and thermal energy. Another horizontal turbulent diffusion parameterisation was implemented and the routine which treats the interaction between the ionised and neutral components in the lower thermosphere was improved. Finally, the radiation scheme was improved taking into account new insights in this topic.

Summarising all characteristics, one can conclude that COMMA-LIM as a mechanistical model provides us with really good climatologies and reasonable tides as well as other planetary waves. So it can be used for studying the middle atmosphere with low timecosts in a good physical quality. Further work on COMMA-LIM is planning on investigating the latitudinal dependence of gravity waves and their influence on the background flow as well as studies for data assimilation to improve the lower boundary conditions and the distributions of meteorological fields in the troposphere.

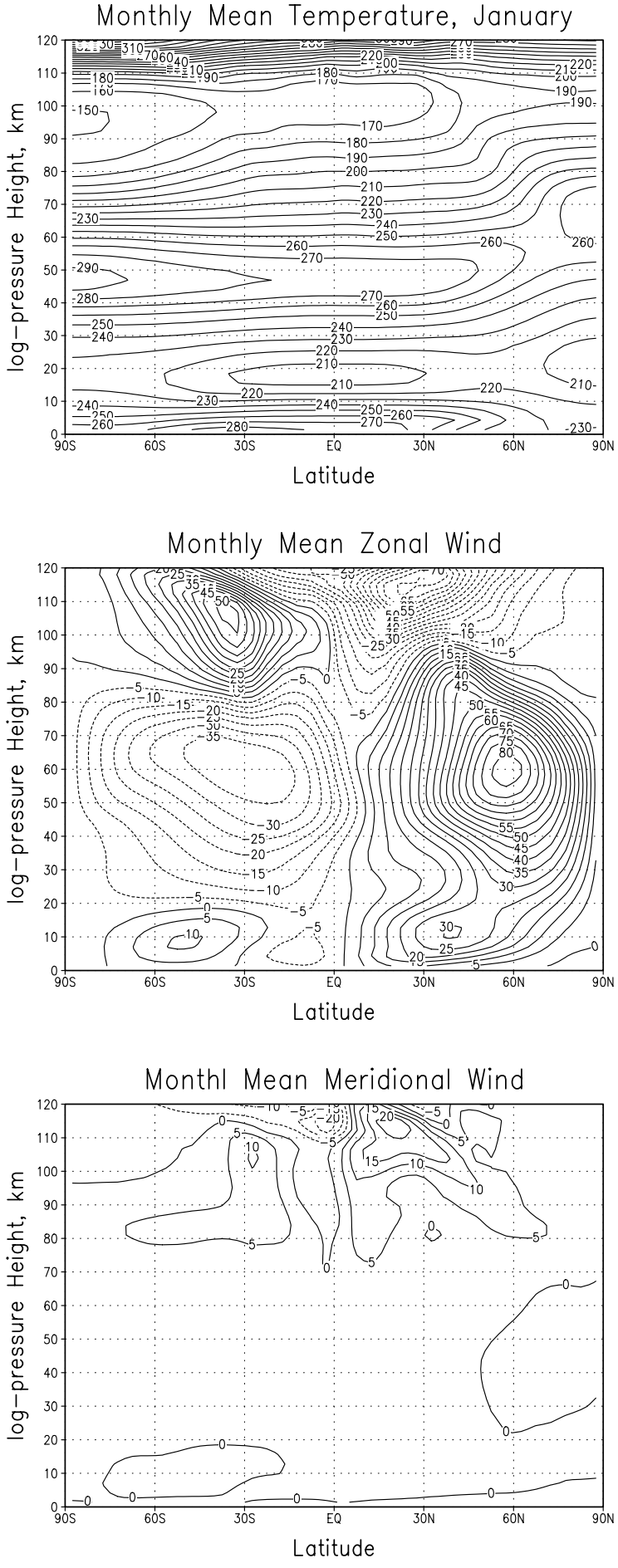

Figure 1: Monthly mean temperature (K) at top, zonal wind (m/s) at mid, meridional wind (m/s) at bottom for January.

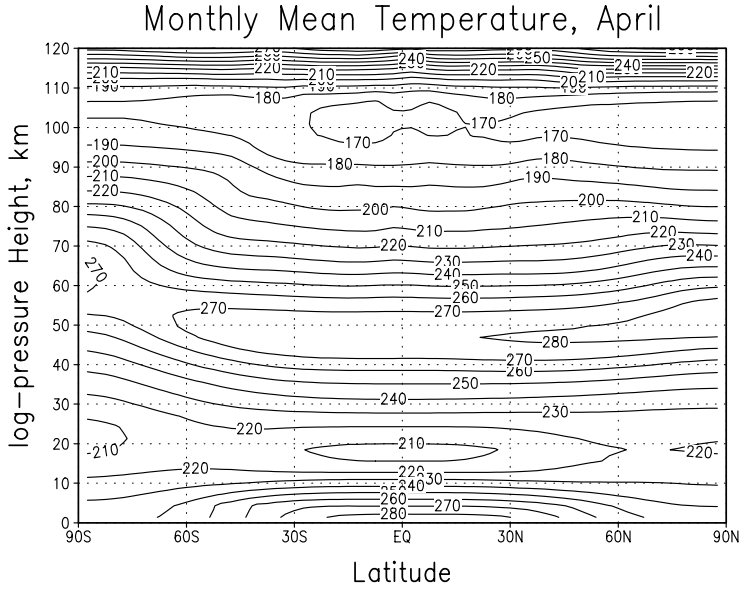

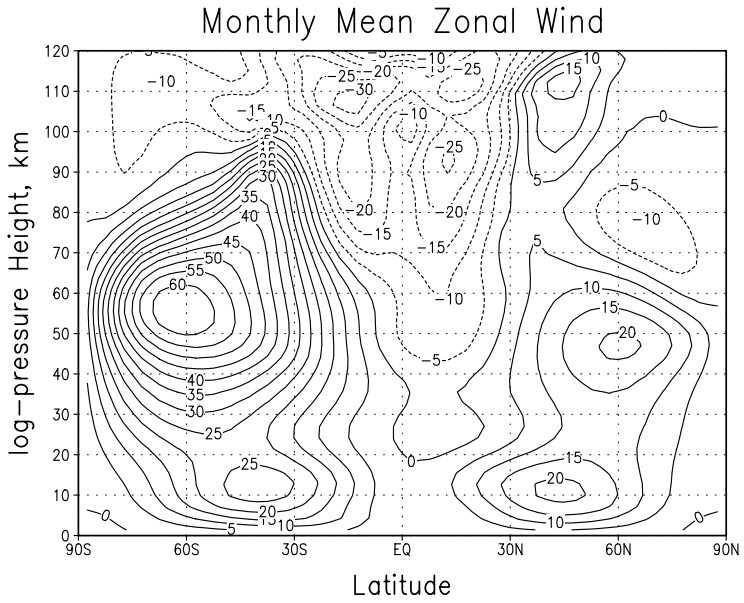

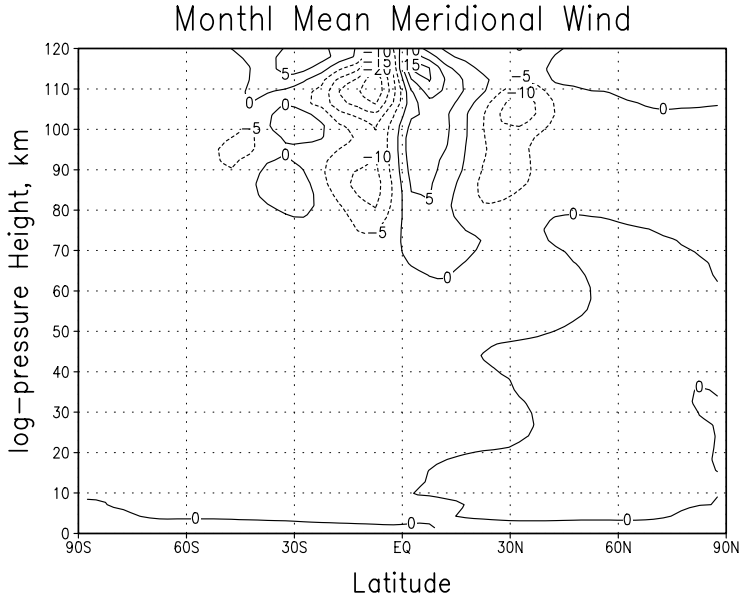

Figure 2: as in Fig.1, but for April.

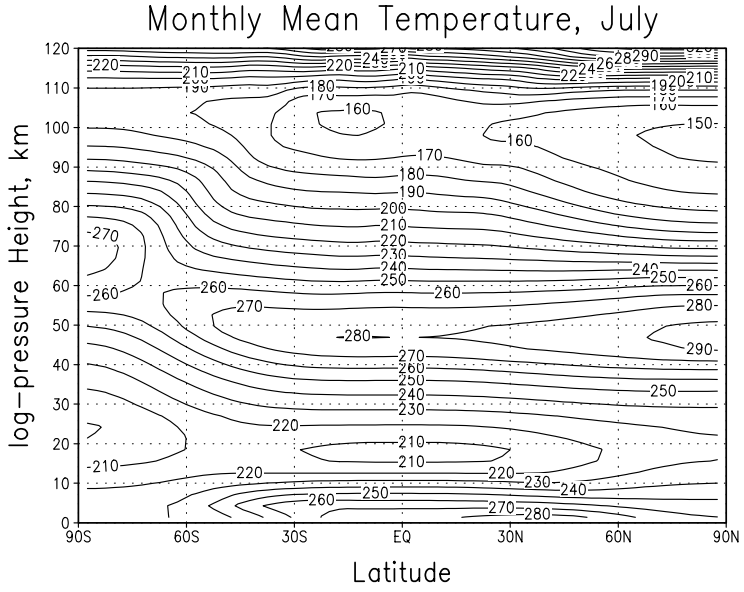

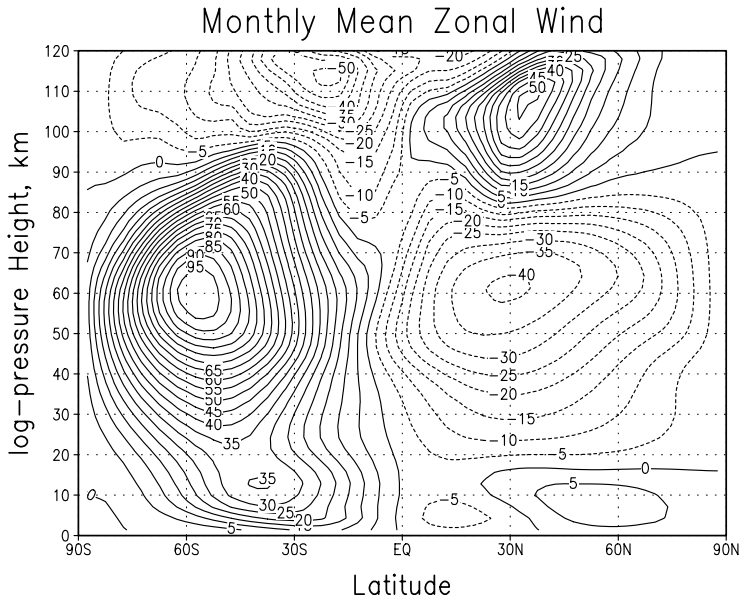

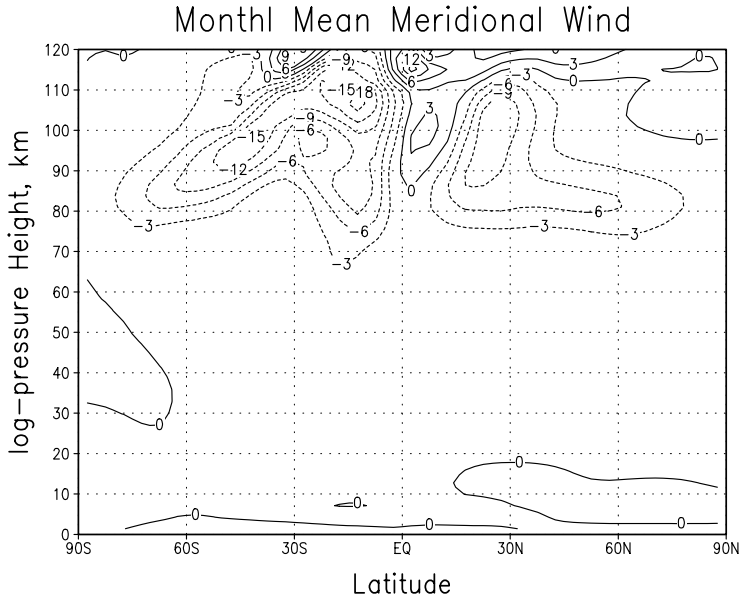

Figure 3: as in Fig.1, but for July.

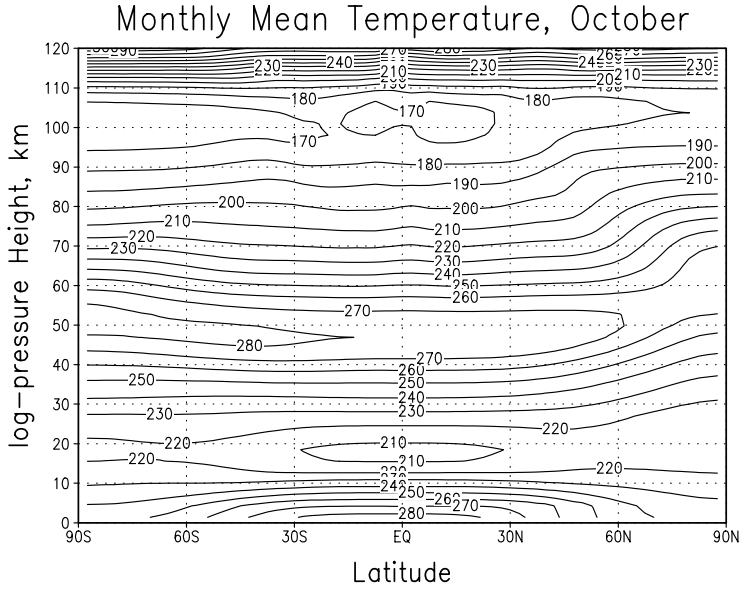

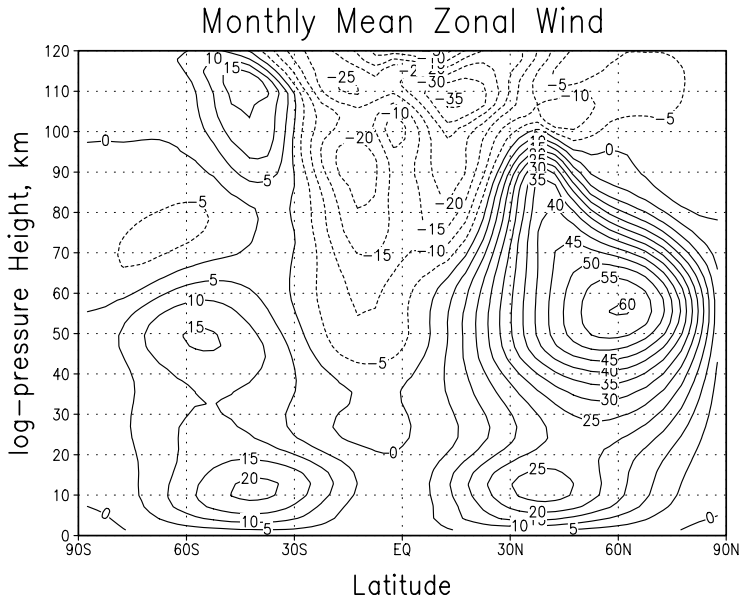

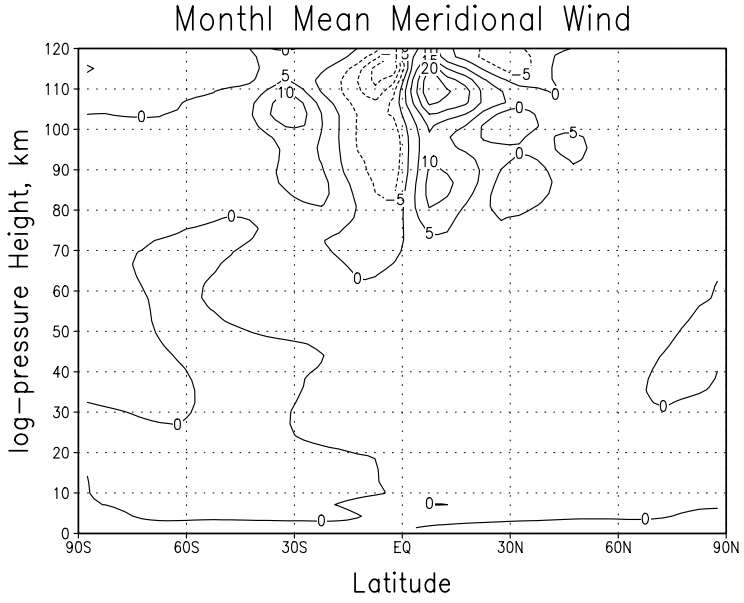

Figure 4: as in Fig.1, but for October.

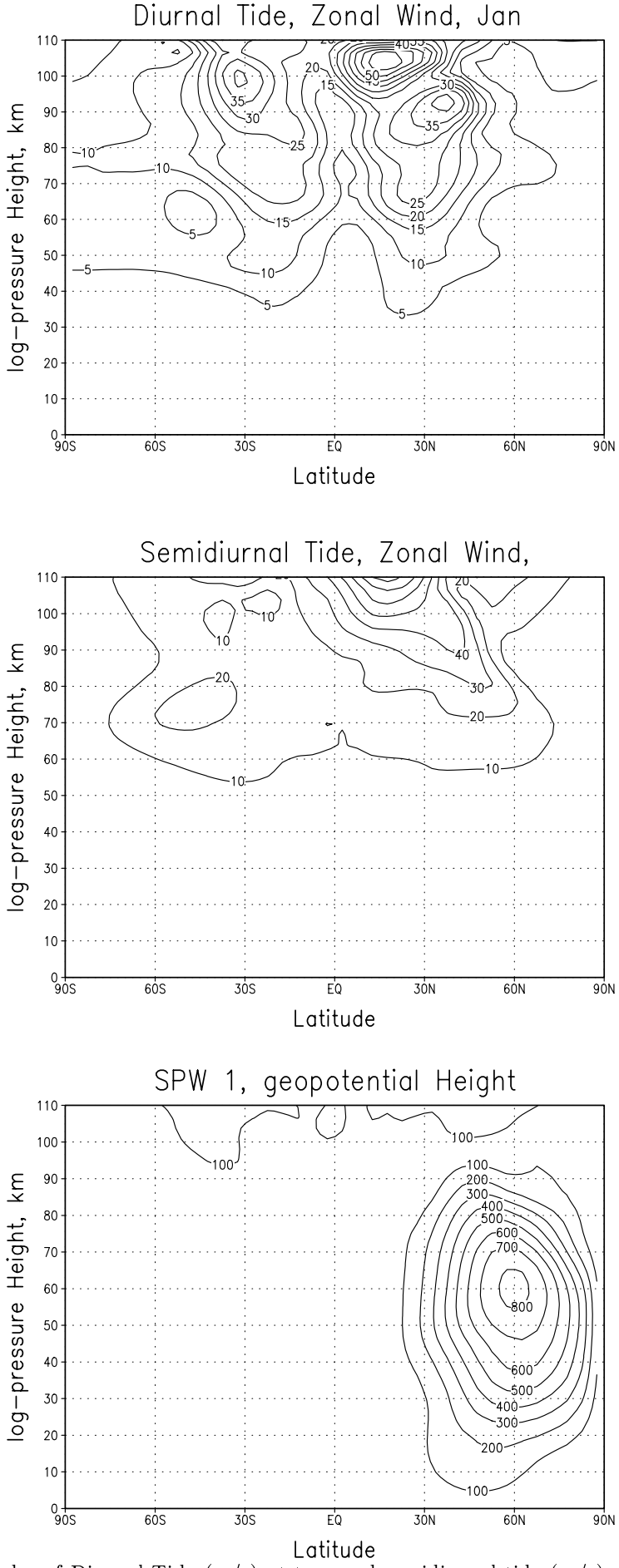

Figure 5: Amplitudes of Diurnal Tide (m/s) at top, and semidiurnal tide (m/s) at mid, both for the zonal wind, and the stationary planetary wave 1 in geopotentail height (gpm) at bottom for January.

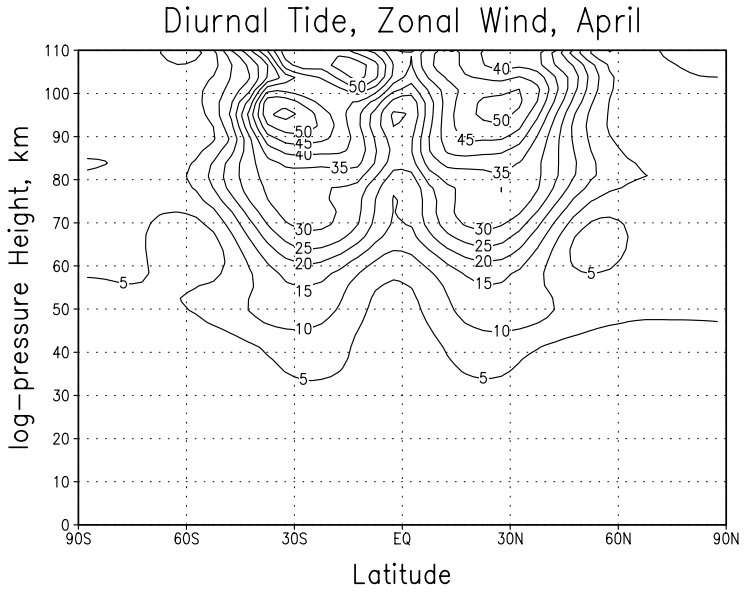

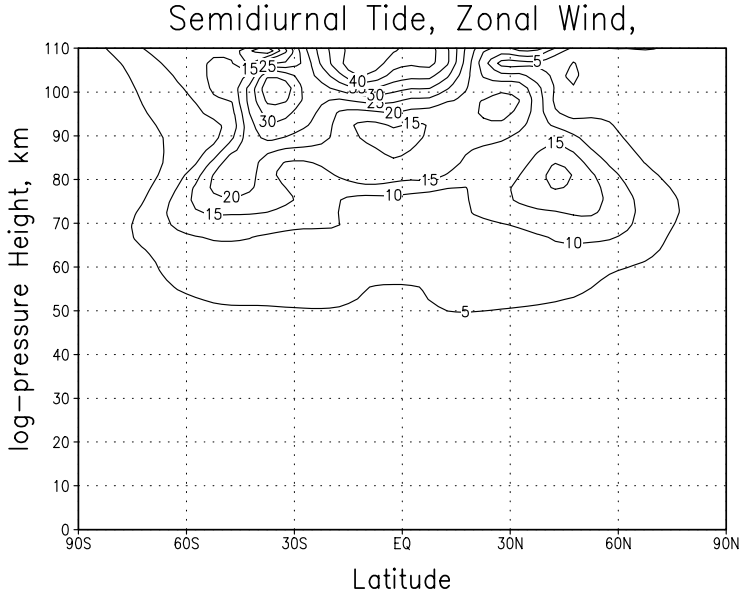

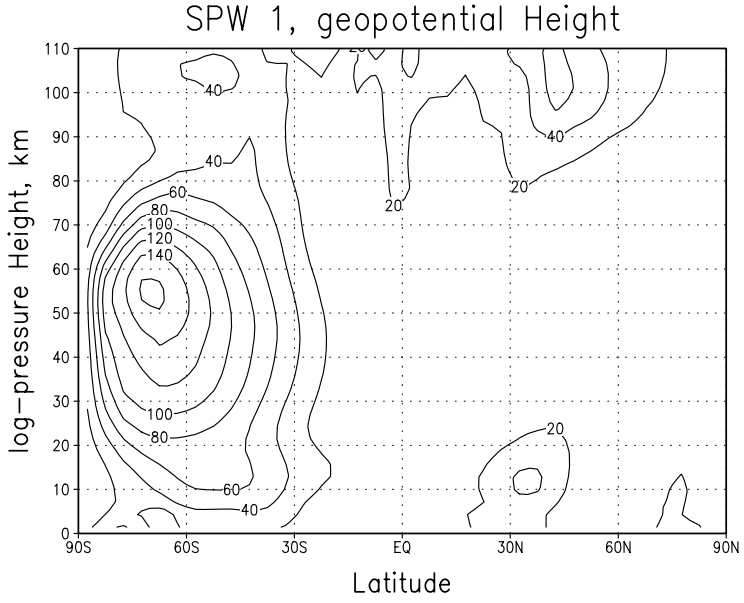

Figure 6: as in Fig.5, but for April

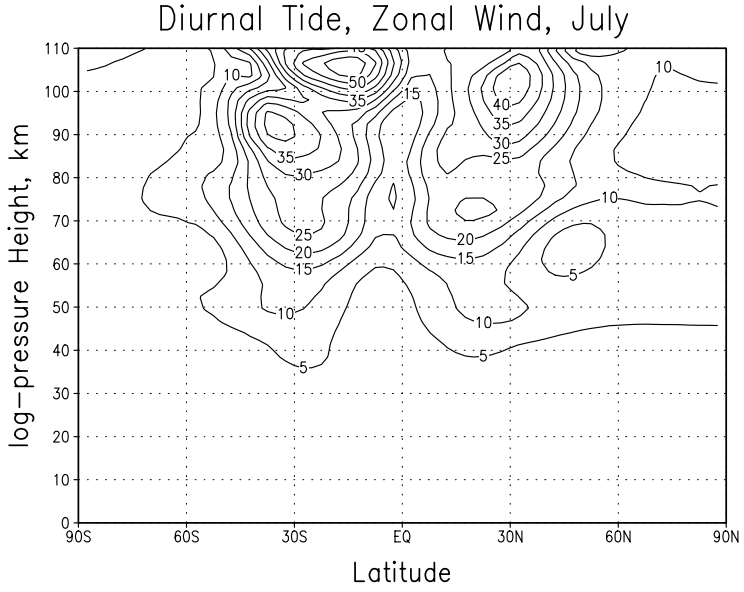

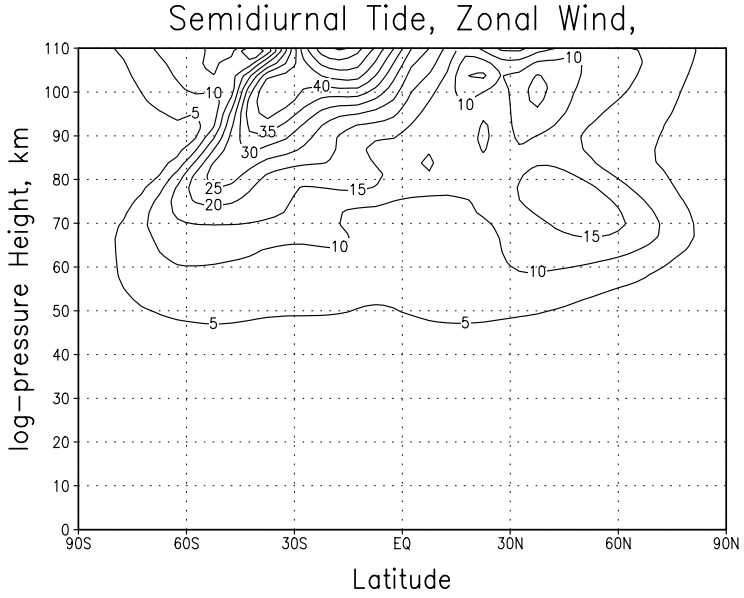

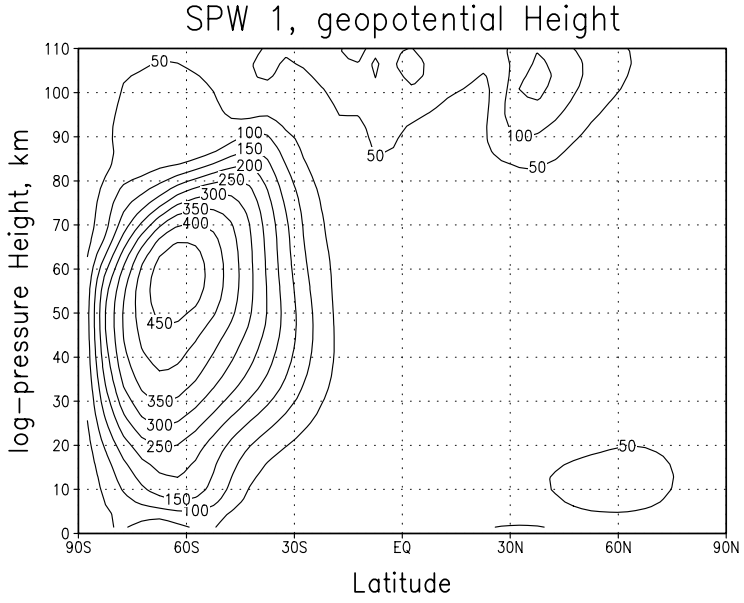

Figure 7: as in Fig.5, but for July

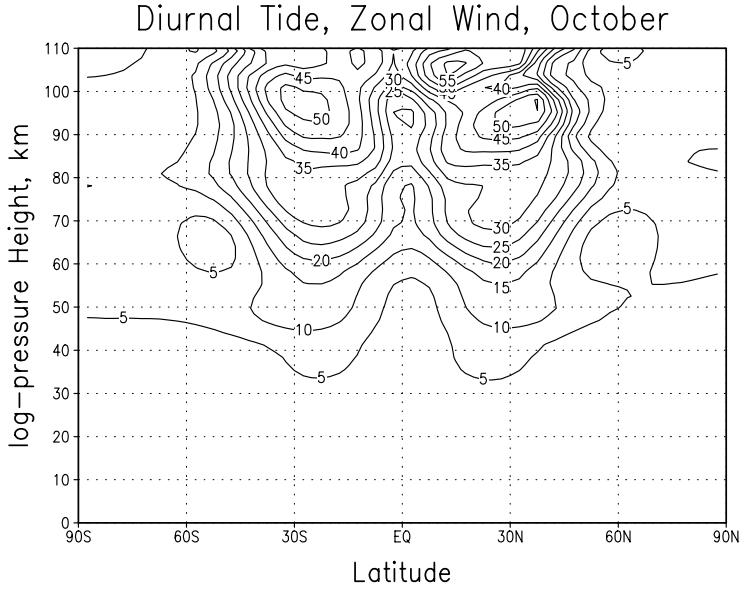

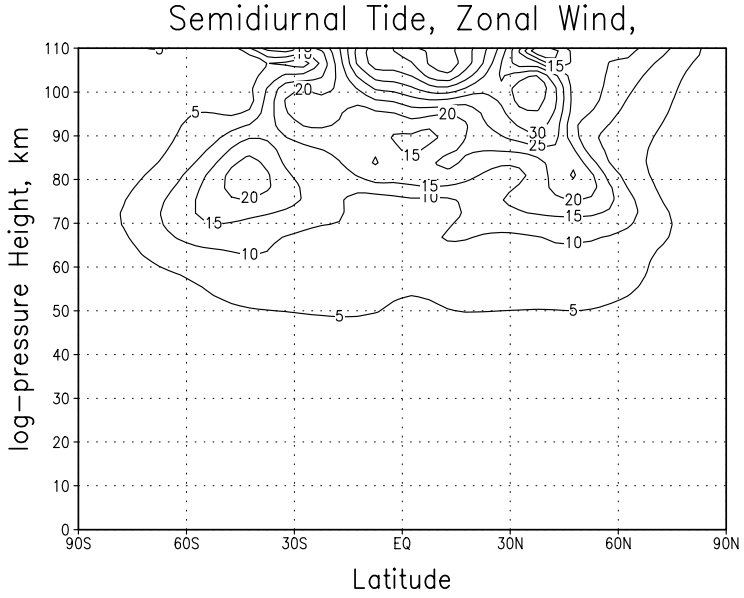

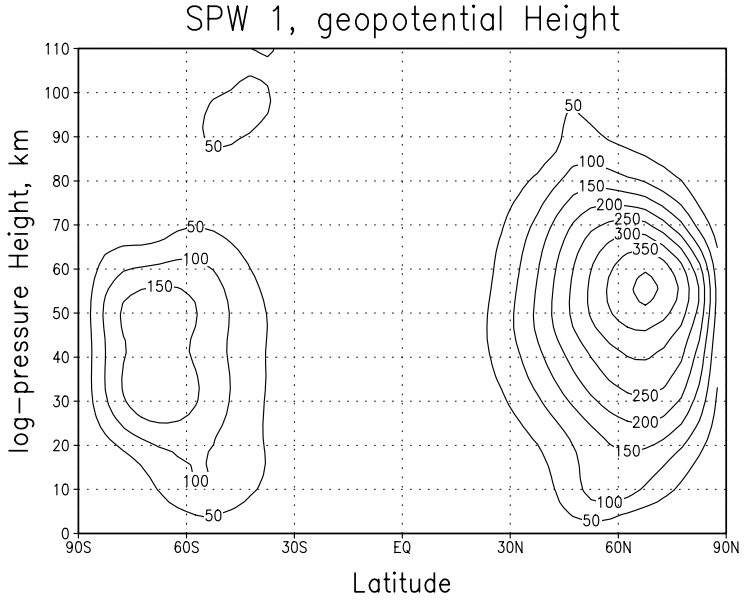

Figure 8: as in Fig.5, but for October

Important Symbols

Symbol	Meaning	Value/Unit
$\mathbf{B}$	geomagnetic field	nT
C	cooling	$K\ d^{-1}$
D	eddy diffusion coefficient	$m^2\ s^{-1}$
$\mathbf{E}$	electrical field	$V\ m^{-1}$
E	GW energy	$kg\ m^{-2}\ s^{-1}$
$\mathbf{F}$	GW energy flux	$kg\ s^{-3}$
H	scale height	$7\ km$
K_m	thermal conduction coefficient	$W\ m^{-1}\ K^{-1}$
K_h	turbulent thermal conduction coefficient	$W\ m^{-1}\ K^{-1}$
K_H	coefficient of horizontal diffusion	$m^2\ s^{-1}$
N^2	Brunt-Väisälä frequency	s^{-2}
R	gasconstant for dry air	$287\ J\ kg^{-1}\ K^{-1}$
Ri_f	dynamical Richardson number	
Pr	turbulent Prandtl Number	3
Q	heating	$K\ d^{-1}$
$\mathbf{V}$	horizontal wind field	$m\ s^{-1}$
W	vertical velocity	$m\ s^{-1}$
a	acceleration	$m\ s^{-2}$
c_p	specific heat of constant pressure	$J\ kg^{-1}\ K^{-1}$
e_{wh}	efficiency of mechanical energy conversion into heat	
g	gravity	$m\ s^{-2}$
$\mathbf{j}$	electrical current density	$A\ m^{-2}$
$k_{x,(z)}$	horizontal (vertical) wavenumber	m^{-1}
k_λ	absorption coefficient	m^{-1}
p, p_0	pressure, reference pressure	hPa
z	height	m
α	Newtonian cooling coefficient	s^{-1}
$\beta_{r\lambda(\varphi)}$	ion drag and Rayleigh friction in zonal (meridional) direction	s^{-1}
ε_b	work against buoyancy force	$m^2\ s^{-3}\ K^{-1}$
θ	potential temperature	K
λ	longitude	
μ	dynamic viscosity	$kg\ m^{-3}\ s^{-1}$
ν	kinematic eddy viscosity	$kg\ m^{-3}\ s^{-1}$
ρ	density	$kg\ m^{-3}$
σ_0	parallel conductivity	$S\ m^{-1}$
σ_1	Pedersen conductivity	$S\ m^{-1}$
σ_2	Hall conductivity	$S\ m^{-1}$
φ	latitude	
ω	frequency	s^{-1}
ω^+	intrinsic frequency	s^{-1}

References

Akmaev, R. A., 2001. Simulation of large scale dynamics in the mesosphere and lower thermosphere with Doppler-spread parameterization of gravity waves. 2. Eddy mixing and the diurnal Tide. *J. Geophys. Res.* ,**102**, 1205-1203.

Andrews, D.G., J.R. Holton, and C.B. Leovy, 1987. Middle Atmosphere Dynamics, *Academic Press, Inc.*

Coy, L., and D.C. Fritts, 1988. Gravity wave heat fluxes: A Lagrangian appoach. *J. Atmos. Sci.,* **45**, 1770-1780.

Ebel, A., 1984. Contributions of gravity waves to the momentum, heat and turbulent energy budget of the upper mesosphere and lower thermosphere. *J. Atmos. Terr. Phys.*,**46**, 727-737.

Forbes, J. M., and H. B. Garett, 1979. Theoretical studies of atmospheric tides, *Geophys. Space Phys.*, p. 1951-1981.

Fortuin, J.P.F., and U. Langematz, 1994. An update on the global ozone climatology and on concurrent ozone and temperature trends.
SPIE, Atmospheric Sensing and Modeling, 2311, 207-216.

Gavrilov, N. M., 1990. Parameterization of accelerations and heat flux divergences produced by internal gravity waves in the middle atmosphere, *J. Atmos. Terr. Phys.*, **52**, 707-713.

Gavrilov, N. M., and G. M. Shved, 1975. On the closure of equation system for the turbulized layer of the upper atmosphere, *Ann. Geophys*, **31**, 375-388.

Gavrilov, N. M., and V. A. Yudin, 1992. Model for coefficients of turbulence and effective Prandtl number produced by breaking gravity waves in the upper atmosphere, *J. Geophys. Res.*, **97**, 7619-7624.

Hodges, R. R. Jr., 1967. Generation of turbulence in the upper atmosphere by internal gravity waves, *J. Geophys. Res.*, **72**, 3455-3458.

Hodges, R. R. Jr., 1969. Eddy diffusion coefficients due to instabilities in internal gravity waves, *J. Geophys. Res.*, **74**, 4087-4090.

Holton, J. R. and X. Zhu, 1984. A further study of gravity wave induced drag and diffusion in the mesosphere, *J. Atmos. Sci.*, **41**, 2653-2662.

Hunt, B. G., 1986. The impact of gravity wave drag and diurnal variability on the general circulation of the middle atmosphere, *J. Meteorol. Soc. Jap.*, **64**, 1-16.

Izakov, M. N., 1978. On the influence of turbulence on a thermal regime of the planetary thermospheres, *Cosmic Research*, **16**, 403-411, 1978, in Russian.

Jakobs, H. J., Bischof, M., Ebel, A., and P. Speth, 1986. Simulation of gravity wave effects under solstice conditions using a 3-D circulation model of the middle atmosphere, *J. Atmos. Terr. Phys*, **48**, 1203-1223.

Khattatov, B.V., M.A. Geller, V.A. Yubin and P.B. Hays, 1997. Diurnal migrating tide as seen by the high-resolution Doppler imager UARS; 2. Monthly mean global zonal and vertical velocities, pressure, temperature, and inferrred dissipation, *J. Geophys. Res.*, **102**, 4423-4435.

Labitzke, K., J. J. Barnett, and B. Edwards (Eds.), 1985. Middle Atmosphere Program, Draft of a new reference middle atmosphere. Handbook for MAP, Vol.**16**.

Lindzen, R.S., 1968. The application of classical atmospheric tidal theory, *Proc. R. Soc. London*, Ser. A, **303**, 299-316.

Lindzen, R.S., 1981. Turbulence and stress owing to gravity wave and tidal breakdown, *J. Geophys. Res.*, **86**, 9707-9714.

Lange, M., 2001. Modellstudien zum CO_2-Anstieg und O_3-Abbau in der mittleren Atmosphäre und Einfluš des Polarwirbels auf die zonale Symmetrie des Windfeldes in der Mesopausenregion. *Wiss. Mitt. d. Instituts f. Meteorologie Leipzig*, **Bd. 25**.

Liou, K.N., 1992. *Radiation and Cloud Processes in the Atmosphere*, Oxford Monographs on Geology and geophysics No. 20, 487 pp., Oxford Univ. Press, New York, Oxford.

Marchuk, G.I., V. Dymnikov, V. Zalesny, V. Lykossov, and V. Ya. Galin, 1984. *Mathematical Modeling of the General Circulation of the Atmosphere and Ocean*, 320 pp., Gidrometeoizdat (in Russian).

McLandress, C., 2002. The seasonal variation of the propagating diurnal tide in the mesosphere and lower thermosphere. Part I: The role of gravity waves and planetary waves, *J. Atmos. Sci.*, **59**, 893-906.

Medvedev, A.S. and G.P., Klaassen, 2000. Parameterization of gravity wave momentum deposition based on nonlinear wave interactions: basic formualtion and sensitivity tests, *J. Atmos. Solar.-Terr. Phys.*, **62**, 1015-1033.

Medvedev, A. S. and G. P. Klaassen, 2002. Thermal effects of saturated gravity waves in the atmosphere, *J. Geophys. Res.*, **107**, in press.

Mlynzak, M.G., and S. Solomon, 1993. A detailed Evaluation of the heating Efficiency in the Middle Atmosphere, *J. Geophys. Res.*, **98**, pp.10517-10541.

Monin, A. S., and A. M. Yaglom, 1975 *Statistical Fluid Mechanics: Mechanics of Turbulence*, vol. **2**, 874 pp., MIT Press, Cambridge, Massachusettes.

Plumb, R. A., 1983. A new look at the energy cycle, *J. Atmos. Sci.*, **40**, 1669-1688.

Pogoreltsev, A. I., 1996. Production of electromagnetic field disturbances due to interaction between acoustic gravity waves and the ionospheric plasma, *J. Atmos. Terr. Phys*, **58**, 1125-1141.

Pogoreltsev, A.I., and N.N. Pertsev, 1996. The influence of background wind on the formation of the acoustic-gravity wave structure in the thermosphere, *Izv. Acad. Sci. USSR Atmos. Oceanic Phys.* **31**, 723-728.

Portnyagin, Y.I., and T.V. Solovjova, 1998. Empirical semidiurnal migrating tide model for the upper Mesophere/lower thermosphere. *Adv. Space Res.*, Vol.**21**, No. 6, 811-815.

Riese, M., D. Offermann, and G. Brasseur, 1994. Energy released by recombination of atomic oxygen and related species at mesopause heights, *J. Geophys. Res.,* **99**, 14585-14593.

Scaife, A.A., J. Austin, N. Butchart, S. Pawson, M. Keil, J. Nash, and I.N. James, 2000: Seasonal and interannual variability of the stratosphere diagnosed from UKMO TOVS analyses. *Q.J.R. Meteorol. Soc.*, **126**, 2585-2604.

Shine, K.P., and J. A. Rickaby, 1989: Solar radiative heating due to absorption by Ozone. *Ozone in the Atmosphere*, ISBN 0-937194-15-8, 597-600.

Strobel, D.F., 1978. Parameterization of the atmospheric heating rate from 15 to 120 km due to O_2 and O_3 Absorption of Solar Radiation, *J. Geophys. Res.*, **83**, 6225-6230.

Swarztrauber,P.N., and A. Kasahara, 1985. The vector harmonic analysis of Laplace's tidal equations. *SIAM J. Sci. Stat. Comput.* **6**, 464-491.

Swinbank, R. and D.A. Ortland, 2001. Compilation of wind data for the UARS Reference Atmospheric Project. $http://code916.gsfc.nasa.gov/Public/Analysis/UARS/urap/$

Zhu, X., 1993. Radiative damping revisited: Parameterization of damping rate in the middle atmosphere. *J. Atmos. Sci.,* **50**, 3008-3021.